Comparative Analysis of Biodiesel Produced from Blends of Palm Kernel Shell and Cocoa Pods Oils with Conventional Diesel Fuel: Characterizations

Bassey NKANANG[1], Fidelis ABAM[2], Macmanus NDUKWU[3], Hyginus UGWU[3], Agnes OBOH[4]

[1]*Department of Mechanical Engineering, Akwa Ibom State University, Ikot Akpaden, Nigeria*
bassynkanang1981@gmail.com

[2]*Department of Mechanical Engineering, University of Calabar, Cross River State, Nigeria*
abamo124@gmail.com

[3]*Department of Agricultural Engineering, and Department of Mechanical Engineering, Michael Okpara University of Agriculture, Umudike, Nigeria*
ndukwu.macmanus@mouau.edu.ng/ugwu.hyginus@mouau.edu.ng

[4]*Department of Mechanical Engineering, University of Uyo, Uyo, Nigeria*
agnesoboh@uniuyo.edu.ng

Abstract*: The uncertainty of predicting the conditions of bio oils for the production of quality biofuels and reusability of catalyst, saving cost of production and time, make characterization of the oils/catalyst imperative. Characterization of bio oils, extracted from palm kernel shell and cocoa pods, the blends, catalyst and biodiesel produced therefrom is investigated. The biodiesel was produced from the hybrid feedstock through the most preferred method known as transesterification. A maximum biodiesel yield of 76.05% was obtained. Titanuim oxide used proved to be efficient catalyst for converting the oil blends to biodiesel. The established results obtained show kinematic viscosity of $5.65 – 7.78\ mm^2 s^{-1}$ @ $40\ ^oC$, density of $0.8428 – 0.8642\ kg/m^3$, cloud point of $4.48 – 6.48\ ^oC$, fire point of $108 – 150\ ^oC$, cetane index of $37.78 – 30.13$, acid value of mg KOH/g, anicidine point of $50 – 46\ ^oC$ etc. All the values fell within the recommended ASTM and EN standards. The Gas Chromatography-Mass Spectroscopy (GC-MS), X-ray Diffractive (XRD), Scanning Electronic Microscopy (SEM), and Fourier Transform Infrared (FTIR) analyses carried out to evaluate the quality of the sample with respect to deterioration, gave an ester percentage of 99.9% for the bio-oil and biodiesel, which is within the minimum standard range of not less than 96.5% recommended. The GC-MS of the blended oil shows that the most prevalent fatty acids identified amongst 13 other distinct compounds were methyl linolenate, methyl palmitate, methyl oleate and methyl eicosadinoate with percentage concentrations of 63.03, 26.9, 8.1 and 2% respectively. The SEM analysis shows high porosity with high specific surface area of the catalyst at magnification of $80 – 269\mu m$; and the FTIR analysis revealed that the functional groups for the bio-oil and blended biodiesel were in range.*

Keywords*: Characterization, Bio-oil, Biodiesel Yield, Titanium Oxide Catalyst, Palm Kernel Shell Oil, Cocoa Pods Oil*

1. INTRODUCTION

The world's oil supplies are running low due to widespread industrial activities and population growth, which have accelerated the energy crisis and environmental damage in recent decades [1]. Natural gas, coal, and petroleum reservoirs are currently the world's main energy sources, needed to satisfy consumers' insatiable thirst [2]. Despite alternative energy sources, fossil fuels will still provide approximately 96% of the energy consumed in transportation in 2021 [3]. The atmospheric release of various poisonous and dangerous compounds originating from fossil fuels is one of the biggest concerns the world is currently facing. This continuous use of fossil fuel contributes to the depletion of the ozone layer [4]. Ozone layer, which is responsible for the absorption of 97 – 99% of the sun's high frequency ultraviolet radiation that causes damage to life form on earth, is depleted through the release of GHGs into the atmosphere [5]. The depletion constitute a serious health risk to human worldwide [4]. This is as a result of human and industrial activities like burning of wastes and internal combustion engines [4, 5, 6, 7, 8]. The activities have increased the emission of CO, CO_2, NO_X, SO_2, and other GHGs globally, into the atmosphere [4, 6, 8, 9, 10]. It has been reported that the damage and injury caused by ground level ozone (O_3) on vegetation have been on the increase over the past half-decade [11]. Combustion of fossil fuels is also a major factor, which has contributed to global warming [12]; and its excessive demand have resulted in the depletion from its reservoirs [13, 14]. Incomplete combustion of fossil fuel reacts with air and water molecules [15]; and its

effect is seen as 'black soot' in some industrial areas or cities [6]. The world's energy needs must be met by finding an alternate fuel because fossil resources are running out daily [16]. This necessitates a serious research to develop a substitute fuel to fossil fuel.

The research is geared towards developing an alternative to fossil fuel, which must be renewable, eco-friendly, locally produced/available, efficient, economically viable, environmentally sustainable and clean. Biodiesel has proven to be one of the best alternative fuels to substitute fossil fuel [6, 17, 18]. The use of biodiesel will help increase global energy efficiency [4]. Emissions from CO_2 and other hazardous gases can also be eliminated or drastically reduced if an alternative source of energy generation such as biodiesel is considered [19]. Since fats from both animals and vegetables have low volatility and high viscosity, they are used to make biodiesel from sustainable biological resources. It also goes by the name fatty acid methyl ester (FAME). It is mostly made by a procedure known as alcoholysis or transesterification. This is the process via which animal fats or oils derived from plants (seeds, vegetables, etc.) combine with short-chain aliphatic alcohol, primarily methanol or ethanol [20]. The high viscosity of the bio-oil is lessened by this production procedure [21, 22, 23]. Trans-esterification is a highly effective method for producing biodiesel. It is the easiest and most economical process recorded [6, 24, 25, 26].

Transesterification permits the vegetable oil esters to be mixed with liquor, subsequently evacuating the glycerides shown in the bio-oil [27, 28]. To quicken the response time and increase the oil yield, a catalyst is used. This catalyst may be homogeneous or heterogeneous. The homogeneous catalyst offers arrangements of preferences; be that as it may, the major impediment is that it cannot be reused [4, 29]. In expansion, an appropriate amount of water is required for washing in order to evacuate the catalyst build-ups. Heterogeneous (strong) catalysts have the points of interest of simple partition from the response medium and reusability [4, 6, 30]. As a result, catalysts that are heterogeneous for transesterification (illustration: biochar and solid-acid-based catalysts) have advanced to demonstrate high efficiency in biodiesel production [31]. They offer other preferences due to their eco-friendliness, multi-production procedures, blending, low cost, non-corrosiveness, and utilitarian surface [6, 32]. Thus, heterogeneous catalyst is considered to be a green process.

Heterogeneous catalyst research and development are becoming increasingly important nowadays [33, 34]. Numerous studies have demonstrated the use of various catalysts (e.g., KOH, NaOH, eggshell, ripe and unripe plantain peels, metal oxides, Zeolites etc.) and feedstocks in the manufacture of biodiesel [6, 24, 25, 26, 34 35, 36, 37, 38]. Other studies to address the challenges associated with biodiesel production using different feedstocks have also been carried out [2, 4, 6, 12, 14, 39].

However, amongst these studies, there are currently limited studies and records of the usage of blends of cocoa pod oil and palm kernel shell oil with titanium oxide as a catalyst. This work looked at the use of nonedible oils from these agricultural wastes, which are in abundant in the Sub-Saharan African countries like Nigeria, as feedstocks in the manufacturing of biodiesel. This will enhance economic growth, environmental safety, wealth creation etc, amongst the local communities, country and world at large. The characterization of these oils and the catalyst that enables their usage in the transesterification process to produce biodiesel were among the objectives of this work. It also looked at employing a heterogeneous nano-catalyst (titanium oxide) to synthesise biodiesel from mixtures of cocoa pods and palm kernel shell oils. Titanium dioxide have shown high potentials as heterogeneous catalyst due to its high surface area, strong metal support interaction, chemical stability, and acid–base property [25].

2. MATERIALS AND METHODS

2.1 Materials

One (1) litre of both palm kernel shell oil and cocoa pods oil, beaker, heater, thermometer, retort stand, round bottom flask, reflux condenser, separating funnel, cotton material, weigh balance, litmus paper, oven, filter paper, nano catalyst (titanium oxide), distilled water, magnetic capsule, soxhlet extractor, n-hexane and carbonizer were utilized for this study.

2.2 Methods

2.2.1 Nano catalyst

The Jules Therapeutic Factory in Lagos, Nigeria provided five (5) kilogrammes of titanium oxide. There are different methods of preparing the nano-particle of the catalyst; of which an example is the co-precipitation method [26]. In order to reduce production cost and protect the environment, the nano catalyst was produced and supplied to the factory in its powdered form. This was done through the use of micro reactors, which is capable of making possible, chemical transformations not feasible with traditional techniques by the producers [25]. After passing through a 500 μm particle size screen, the catalyst was submerged in the distilled water. The catalyst, or lower section, was separated from the undesired particles (which float on the water) after it was submerged in the water for 120 minutes. To ensure that the catalyst sample was free of any contaminants, the water portion that was covering it was carefully drained off. To dry it out, the catalyst was placed in an oven set to 60 ^{0}C for 120 minutes.

2.2.2 Oil extraction by soxhlet method

Palm kernel shell and cocoa pods obtained from the parent fruits in Onna, Akwa Ibom and Ogoja, Cross River States respectively were air dried and sorted to remove impurities. Both feedstocks were ground using industrial blender, and 100g of the ground seeds was measured into a semi-permeable cloth material.

Figure 1: Titanium oxide in powdered form

This weighed ground seed in the cloth material was inserted into the thimble of a Soxhlet extractor (500ml); while n-hexane of 400ml was measured into the 500ml flat bottom round flask. The sample was deposited in the semi-permeable material inside the Soxhlet extractor and linked to a condenser that was attached to the round flask with a flat bottom that contained the n-hexane. The whole system was heated up on a hot plate; and water was made to go round the condenser via the outer jacket. Oil extractions from the sample was terminated when no further oil could be extracted. The raw sample (after extraction) in the semi permeable material was disposed; and the n-hexane mixture and oil remaining in the flat bottom flask were separated by distillation process. Here, the n-hexane, which was on top, was distilled over, and the oil (under), was allowed to remain in the flask.

Figure 2: Experimental set up for oil extraction (Soxhlet method)

2.3 Oil Characterization

To determine the acidity, moisture content, peroxide, saponification, iodine, viscosity, density, and refractive index of the palm kernel and cocoa pod oils, the following techniques were used;

2.3.1 Density

The weight of an empty beaker was recorded. Afterwards, 100ml of the sample was measured into a 50ml density beaker. The weight of the sample together with the density bottle was also recorded. After that, the actual weight of the sample was determined by subtracting that of the empty beaker from the total weight of sample and the density bottle. From the results obtained, the ratio of the weight of the oil to the volume of the oil, as shown in Equation 1, was used in calculating the density of the oil.

$$SG = \frac{W_S}{V_S}$$

(1)

Where: SG = specific gravity, Ws = sample weight and Vs = sample volume.

2.3.2 Refractive index

The oil refractive index was determined using a digital table top refractometer (HI96800) manufactured by Hanna Instruments, Romania. The device was initially calibrated to zero using distilled water. The sample was later placed on a glass prism for the readings to be taken.

2.3.3 Moisture

With the use of dry oven method, the moisture content was calculated according to Agbede, O. [37]. Ten (10) g of the oil sample was introduced into an already weighed petri-dish (designated "a"). The petri-dish sample was placed in an oven set to 120^0C and left for an hour. This was placed in a desiccator to chill. After the sample was heated in the oven, its second weight (designated "b") was measured. The percentage moisture then was calculated using Equation 2.

$$\% \text{ moisture} = a - \frac{b}{W_s} (100) \tag{2}$$

2.3.4 Saponification value

Saponification value was determined according to the method of Boerlage, G. and Broeze, J. [27]. The amount of potassium hydroxide (KOH) in milligrams required to neutralize the fatty acids produced by fully hydrolyzing one gram of the sample is known as saponification [6]. 100 ml of 0.8N ethanolic KOH was added to one (1.0) g of the sample, which had been weighed into a conical flask. To saponify the sample, the mixture was refluxed. Three drops of phenolphthalein was used as indicator to titrate the unreacted Potassium hydroxide (KOH) back, with 0.8N hydrochloric acid. Equation 3 was used to determine the sample's saponification value.

$$\text{Saponification value} = \frac{(T_V) (N_{Hcl}) (56.1)}{(W_S)} \tag{3}$$

Where: Tv = titre value, N_{Hcl} = normality of Hcl and 56.1 = molecular weight of KOH.

2.3.5 Viscosity

The kinematic viscosity was measured using a Poulten Selfe and Lee Ltd. U-tube viscometer (PSL ASTM-IP 350). The sample was added to the viscometer using a micropipette. The sample flow time was determined in seconds at 60 ^{0}C using Equation 4.

$$\text{Kinematic viscosity} = c\, t\ (\text{mm}^2\text{s}^{-1}) \tag{4}$$

Where: c is viscosity constant = 0.4891 and "t" is the time for the measurement.

2.3.6 Acid value

This is defined as the number of milligram of Potassium hydroxide (KOH) needed to neutralize the FFA in 1g of sample. Three drops of phenolphthalein indicator was introduced into a conical flask, which contained 0.5 g of the sample and 25ml of ethanol. The solution was titrated while being shaken constantly until a faint, pink colour appeared, and persisted for 60 seconds. The volume of the titrated solution at end was recorded. From the results obtained, the acid value was calculated from Equation 5.

$$\text{Acid Value} = \frac{(T_V)(N_{KOH})(5.61)}{(W_S)} \tag{5}$$

Where: N_{KOH} = normality value for KOH and 5.61 = molecular weight of KOH by 10.

2.3.7 Peroxide value

Using the methodology described in [27], the peroxide value was calculated. The peroxide value can be defined as the measure of peroxides present in the oil sample. Fresh oils usually have peroxide values well below 10mEq/kg; and a rancid taste is often noticeable when the peroxide value is between 20 and 40 mEq/kg [6]. A conical flask weighing one (1.0) g of the oil sample was filled with 30 ml of a mixture of glacial acetic acid and chloroform in a 2:1 ratio. Thereafter, one milligram of 10% potassium iodide (KI) was added to the mixture. The mixture was shaken vigorously, covered and kept in the dark for 2 minutes; and 55ml of starch indicator added. Approximately 0.02N sodium thiosulphate solution was used to titrate the entire solution. The peroxide value was determined from Equation 6.

$$Peroxide\ value = \frac{(100)(V_1 - V_2)(N_t)}{W_S} \tag{6}$$

where Nt = normalcy of the titrant = 0.02 of sodium thiosulphate solution; V_1 = titre value of the sample; V_2 = titre value of the blank; and 100 = milliequivalent conversion factor.

2.3.8 Iodine value

Iodine value was determined according to the method of Boerlage, G. and Broeze, J. [27]. The iodine value of a sample is defined as the weight of iodine absorbed by 100 parts by weight of the sample. One and a half grams (1.5) g of the oil sample was weighed and 20ml of chloroform added. Afterwards, 25ml of Wiji's solution was added and mixed vigorously. The solution was tightly covered before being placed in a dark environment for 60 minutes. 25ml of 10% KI with 200ml of distilled water was also added. The solution was allowed to undergo a chemical reaction until it turned red. 5 ml of 5% starch solution indicator was added, and watched as the solution's colour changed to blue-black. After that, the solution

was titrated with a 0.1N thiosulphate solution until black precipitates showed up in the colourless solution. Iodine value was then determined, using Equation 7.

$$Iodine\ value = \frac{(12.69)(V_1 - V_2)(N_t)}{W_S}$$ (7)

Where: 126.9/10 = 12.69 = molecular weight of iodine in g/mol, V_1 = titre value of the sample, V_2 = titre value of the blank, and Nt = normality of titrant = 0.1N sodium thiosulphate solution respectively.

2.4 Characterization of the Nano Catalyst

In order to be used as catalysts for biodiesel production, the nano catalyst was characterized for the following properties:

2.4.1 pH

The pH of the samples was determined using pH meter (Model pH-206) manufactured by Metler Toledo (seven compact series). Five (5) g of the samples were weighed and dissolved in 50ml of distilled water. The Samples were properly dissolved in solution using a glass rod, and the pH meter calibrated using pH buffer solutions before use.

2.4.2 Bulk density

A 50 ml density vial (pycnometer) was used to measure bulk density. The original weight of the empty pycnometer was "w_1" The test sample was continuously tapered until the pycnometer could hold no more samples, after being filled up to the neck. It was weighed and recorded as "w_2" at that time. Equation 8 was used to compute bulk density.
.

$$Bulk\ denity = \frac{w_2 - w_1}{V_S}$$ (8)

2.4.3 Surface area

The surface area of the test sample was determined. One and a half grams (1.5) g of activated carbon was dissolved in 200ml of Hcl. After that, 30g of NaCl was added and the suspension stirred vigorously. The volume was then made up to 250ml with de-ionized water as the pH changed to 4.0, and 0.10N NaOH used to increase the pH to 9. The surface area was then calculated using Equation 9.

$$S\left(\frac{m^2}{g}\right) = 32V - 25$$ (9)

where: S = the surface area (m^2/g), V = volume of NaOH used to increase the pH, and 25 is the Saers constant.

2.4.4 Percentage carbon

Five (5) g of the test sample was weighed into a 250 ml conical flask, and 10ml of 0.167M $K_2Cr_2O_7$ was added. Also, 20ml of concentrated sulphuric acid was added and swirled properly to permit mixing and allowed to stand for about 60 minutes. The solution was diluted with 400ml of distilled water to make the solution clear for viewing during titration and 10ml of 85% phosphoric acid added. Since the phosphoric acid and sodium fluoride are complex Fe^{3+} which would interfere with the titration end point; 10 drops of ferroin indicator was thus added and the whole solution titrated with 0.5M iron (II) sulphate to a burgundy (red or white unblended) endpoint. Hence, the percentage carbon and the percentage organic matter were determined by Walkley Black method [40], using the Equations 10 and 11 respectively.

$$\%\ Carbon = \frac{(B - S) \times M\ of\ Fe^{2+} \times 12}{g\ of\ oil \times 4000} \times 100$$ (10)

where: B = ml of Fe^{2+} solution used to titrate blank, S = ml of Fe^{2+} solution used to titrate sample, and $^{12}/_{4000}$ = milliequivalent weight of C in g.

$$\%\ Organic\ matter = \frac{\%\ total\ C \times 100}{58}$$ (11)

2.4.5 Volatile matter

The components in biodiesel that can evaporate at comparatively low temperatures are referred to as volatile matter. It is primarily composed of water, unreacted esters, and leftover methanol. The nano sample weighed five (5) grams and was placed into a ceramic crucible. After being put within a muffle, it was heated to 350^0C. The furnace was removed and weighed once again after being allowed to cool to 150^0C. Next, using Equation 12, the percentage of volatile matter was determined.

$$\%\ Volatile\ matter = \frac{lost\ in\ weight\ due\ to\ moisture\ and\ V.M.}{weight\ of\ sample} \times 100$$ (12)

2.4.6 Particle density

Distilled water was poured into a cylindrical measuring cylinder to 50ml mark, and 10g of nano sample introduced into the measuring cylinder. The volume of displaced water was noted and the particle density and total porosity determined using equations 13 and 14 respectively.

$$Particle\ density, \rho_p\ (gcm^{-3}) = \frac{M_S}{V_{wd}} \quad (13)$$

$$Total\ porosity\ (\%) = 1 - \left[\frac{\rho_b}{\rho_p}\right] 100 \quad (14)$$

Where: M_S = mass of sample, V_{wd} = volume of water displaced, ρ_b = bulk density, and ρ_p = particle density.

2.5 Biodiesel Production (Transesterification) and Characterization

2.5.1 Transesterification

According to Samuel [6], Claudia *et al.* [25] and Falowo *et al.* [26], trans-esterification is a highly effective, easiest and most economical method of biodiesel production. It involves the reaction of triglycerides (TG) with alcohol, commonly methanol, into fatty acid methyl esters (FAME) with or without the presence of a base, acid or enzymatic catalyst. Four types exist; but the most common is the base-catalyzed transesterification, because of its fast reaction time, improved yield, mildest reaction condition, low cost, low corrosiveness, and low toxicity [41]. Parameters like reaction time, molar ratio, and catalyst dosage have been found to impact biodiesel yield [4, 42]. Increasing oil yield and lowering production costs can be achieved by optimising these variables [6, 43]. It can produce up to 98% oil yield at moderate temperatures, pressure and reaction time [44]. Biodiesel was produced through this production process from the pre-treated blends of PKS and CP oils in a spherically-shaped glass reactor with three (3) necks and a round bottom. The high free fatty acid of the oil blend was reduced via the esterification reaction.

The procedure for producing biodiesel from the pre-treated esterified blends of PKS and CPs oils was carried out in the lab using the reactor. This reactor created the methyl ester or biodiesel. The amount of methanol and catalyst to be added for each experiment cycle was determined. It was also decided how much sample oil would be used in each round. After that, the catalyst and methanol were added to the sample oil and thoroughly mixed to allow the catalyst to dissolve. 50ml of the mixture of cocoa pod and palm kernel oils was added to the three-necked reactor once it had properly dissolved.

The mixture was placed on a magnetic heating mantle. Before the heater was switched on, a reflux condenser, which has chamber for cold water to be circulated round, was connected to the middle neck of the reactor. Mercury in glass thermometer was also connected to the right hand neck of the reactor. A plastic bung was used to hold the thermometer. Through the left neck of the reactor, a stirring nob, which has the shape of a capsule was inserted into the reactor; and closed with a plastic bung. The heater was switched on and maintained at an established speed, while regulating the temperature as required. The reaction was carried out for different temperatures at a required time. At the end of the transesterification process, the product was allowed to remain in the separating funnel for twelve (12) hours, so that it could settle for easier separation of the glycerol. The separation funnel was afterwards opened through the tap, for the crude glycerol, which stays below, to go out first, while the methyl ester (biodiesel), which was on top, was left behind.

2.5.2 Characterization of biodiesel

i. Density, Moisture Contents, Viscosity, and Acid value parameters of the Biodiesel produced: The methods adopted in determining these parameters for the bio-oil sample expressed in Equations 1, 2, 4 and 5 respectively, were used to obtain the corresponding values for the biodiesel sample that was produced.

ii. Anisidine point: Biodiesel and anisidine oil are immiscible substances at certain temperatures. To determine the anisidine point of the biodiesel, a certain volume of the anisidine oil was poured into a test tube, and the same volume of biodiesel sample was also introduced into the test tube. The samples were immiscible, and they formed double phase. It was carried into a refrigerator. After a certain period, the samples mixed together. The least temperature at which they mixed was recorded as the anisidine point.

iii. API gravity: This was obtained from the specific gravity of each product according to Rajarshi *et al.* [39], as expressed in Equation 15.

$$API = \left(\frac{141.5}{SG\ at\ 60^0\ F}\right) \quad (15)$$
Where: SG = specific gravity of the fuel

iv. Diesel index: The diesel index is determined by the ignition quality of the fuel [45, 46]. Higher diesel index enables easy start of a diesel engine. According to Rajarshi *et al*. [39], the diesel index was calculated from Equation 16.

$$Diesel\ index = \frac{AP\ (°F) \times API\ Gravity}{100} \quad (16)$$
Where: AP = anisidine point

    v. Cetane number: This is expressed according to Rajarshi *et al.* [39] as:

$$\textbf{\textit{Cetane number}} = \text{diesel index} - 3 \tag{17}$$

   vi. Gross calorific value: This is given by Agbede, O. [37] in Equation 18, as:

$$GCV = 12400 - 2100 \times \rho^2 \tag{18}$$

     Where: GCV = gross calorific value, and ρ = density of fuel

  vii. Flash point and fire point: The flash point is the lowest temperature which fuel ignites when light source is brought close to it; and fire point is the lowest temperature which the fuel combusts continuously when light source is brought to it [27]. To determine these fuel properties, the diesel sample was poured into a glass dish until it covered the surface of the dish. After, a mercury-in-glass thermometer was held into the diesel sample, to touch the tip, with the help of a retort stand. This was heated gradually using the laboratory heater while a light source was applied at intervals. The temperature at which the sample continually ignites was identified as the fire point; the temperature at which it ignites and explodes was identified as the flash point.

 viii. Cloud and pour points: The temperature at which the diesel forms mass substances at the surface is known as the cloud point; and that in which it solidifies or forms substances like wax is called the pour point [47, 48]. To determine the cloud and pour points of the diesel sample, it was poured into a test tube. The sample in the test tube was put into a refrigerator; and its temperature was monitor with the help of mercury in glass thermometer. The cloud point was recorded at the temperature where mass of colloids were formed on the sample; while the pour point was recorded when the sample became solidified.

  ix. Fourier transforms infra-red spectrometry (FTIR): FTIR identifies the chemical bonds in the biodiesel molecule by producing an infra-red absorption spectrum. As an effective analytical instrument, the test was used to determine the available functional groups existing in the produced biodiesel and characterizing the covalent bonding information [4, 49].

   x. Gas chromatography-mass spectrometry (GC/MS) Analysis: GC/MS is an analytical method by which complex mixtures of compounds is identified, separated and quantified. The GC/MS test was used to determine the FFAs profile of the starting oils (bio-oil), methyl esters (biodiesel produced) and the unconverted fatty acids in the optimal biodiesel yield using gas chromatography [25].

  xi. Scanning electronic microscopy (SEM): The SEM analysis was carried out to determine the morphology, particle size and internal micro-structure of the catalyst using the principle of light. The test was performed with an electron beam focused on the sample (titanium oxide) to produce the high specific structure of its image [4].

  xii. X-ray diffraction analysis (XRD): The XRD analysis was carried out to determine the crystal structure of the nano catalyst (titanium oxide). In this technique, the X-ray from the source on the sample was diffracted at an angle using the detector while the intensity of the X-rays leaving the sample was measured. The diffraction data was recorded. The intensity of XRD peaks reflects the crystalline nano particles [50].

3. RESULTS AND DISCUSSIONS

3.1 Characterization of Cocoa Pods and Palm Kernel Shell Oils

Table 1: Results of the characterization of cocoa pod and palm kernel shell oils compared with other works

Parameters	Cocoa pods oil		Palm kernel shell oil	
	Values Obtained	Akinola *et al.*, 2018 [51]	Values obtained	Samuel *et al.*, 2024 [4]
Refractive index @ 29°C	1.460	-	1.451	1.466
Moisture (%)	1.15	14.43	0.03	4.23
Density (g/ml)	0.31	0.95	0.879	0.927
Kinematic viscosity @ 40°C (mm^{2}s^{-1})	1.81	1.79	112.76	-
Flash point (^{o}C)	287	-	264	247
Fire point (^{o}C)	308	-	259	259
Cloud point (^{o}C)	-	-	19	19.50
Pour point (^{o}C)	-	-	20	15.00
Oil yield (%)	16.7	-	18.83	17.83
Acid value (mgKOH/kg)	0.45		21.09	
Saponification (mgKOH/kg)	190	-	229.6	220.10
Peroxide value (mEq/kg)	4		1.76	0.87
Molecular weight (g/mol)	686.24	-	766.76	766.76
Volatile matter	57.63	58.75	73.01	-
Ash (%)	6.78	6.99	5.12	-

The characterization of the feed bio-oils gotten from cocoa pods and palm kernel shell and its blend helps to predict the actual condition of the oils; if it has the qualities to produce biodiesel. Table 1 presents the summary of the results obtained from the characterization of cocoa pods and palm kernel shell oils compared with other authors' work separately. From Table 1, oil yield of 16.7 and 18.83% by weight were respectively obtained from the cocoa pods and the palm kernel shell. The oils had peroxide values of 4 and 1.76 mEq/kg, which were considered to be low and good, since the deterioration would be minimal when stored. The result is consistent with the report, which states that oil deterioration is classified as low when the peroxide value falls between 1.0 and 5.0 mEq O_2 kg^{-1} of oil, moderate when it falls between 5.0 and 10.0 mEq O_2 kg^{-1} of oil, and high when it surpasses 10 mEq O_2 kg^{-1} of oil [52]. In order to determine how easy a sample could be used for biodiesel production, the acid value is one of the most important oil quality parameter to consider. High FFA content in the oil is indicated by a high acid value. FFA levels in oil can increase when it is exposed to high temperatures (during frying) or oxidation, which can happen when peroxides or light are present [52]. From the results, the acid values obtained for the cocoa pods and palm kernel shell oils were 0.45 and 21.09 mgKOH/kg respectively.

The hydrolysis of the triglyceride (oil) using a solution of ethanoic alkaline is applied in the determination of its saponification value. The saponification and acid values of the oil sample are two essential properties used in quantifying oil ester percentage and molecular weight. While the molecular weight of the ester is used in determining the quantity of methanol needed for the transesterification process, percentage of ester is the property that helps determine how the triglyceride can be converted to methyl ester. The saponification values obtained were 190 and 229.6 mgKOH/kg respectively. Before biodiesel production, it is necessary that moisture content of the oil been used as feed stock be reduced considerably. This is because much moisture in the oil will hinder or limit the method for biodiesel production.

Table 2 shows selected proximate and ultimate analysis of the blended feedstocks oils compared to bio-oil specifications. From Table 2, the proximate and ultimate analysis results obtained for the blended feedstock (bio-oil), are within the range of the standard bio-oil specifications.

Table 2: Proximate and ultimate analysis of the blended feed stocks oil for selected properties

Parameters	Standard bio-oil specifications [53, 54, 55, 56, 57, 58]	Blended feedstock oil value
Moisture (%)	0.1 – 39	1.16
Density (g/ml)	1.038 – 923.6	0.878
Kinematic viscosity @ $40^{o}C$ (mm^2s^{-1})	40 – 140	56.45
Flash point (^{o}C)	> 39	264
Pour point (^{o}C)	-31.7 – 4	-18
Iodine value (mg/100g)	64.0	38
Specific gravity	0.94 – 1.09	0.94
C	15.75 – 63.56	42.46
H	8.53 – 8.89	6.34
N	0.3 – 3.6	1.67
S	0.11 – 1.49	0.376
O	23.74 – 75.01	66.56
HC	0.1 - 1.68	0.133

3.2 Catalyst Characterization

Characterization of the catalyst is very important in predicting the oil conditions. It also helps determining the usability of the catalyst as material for the production of biodiesel. Table 3 shows the characterization results for titanium oxide nano catalyst. From Table 3, the results show the moisture content, pH, bulk density, volatile matter etc. of the catalyst to be 2.07%, 3.97, $0.76gcm^{-3}$, 9.84% etc. respectively. The catalyst enabled increased reaction rate and was very stable [6, 45]. The titanium oxide was very effective in the production of the biodiesel.

3.3 FTIR/SEM/EDX, GC-MS AND XRD Analyses Results of the Cocoa Pods Oil, Palm Kernel Shell Oil, Biodiesel and Nano Catalyst

3.3.1 Fourier transform Infra-red analysis

The FTIR analysis, used to determine the functional groups in the cocoa pods oil, palm kernel shell oil and the produced biodiesel is shown in Figures 1, 2 and 3 respectively. The largest peak indicates a powerful absorbance at a wavelength of 1100 to 1050 cm^{-1} for cocoa pods oil, 1400 – 1100 cm^{-1} for palm kernel shell oil and 1400 – 800 cm^{-1} for the produced biodiesel; which was related to C-O bonds at the finger print region and C=O ranging from 1500 –$1200.4cm^{-1}$ and 2200 – 2250 cm^{-1} for the produced biodiesel and 2200 for the palm kernel shell oil.

Table 3: Catalyst characterization

Parameter	Titanium oxide nano catatlyst
Moisture (%)	2.07
Bulk Density (g cm^{-3})	0.76
pH	3.97
Surface Area (m^2 g^{-1})	112
Organic Carbon (%)	3.71
Volatile matter (%)	9.84
Particle Density (g cm^{-3})	3.6
Total porousity (%)	44.27
Ash (%)	4.54
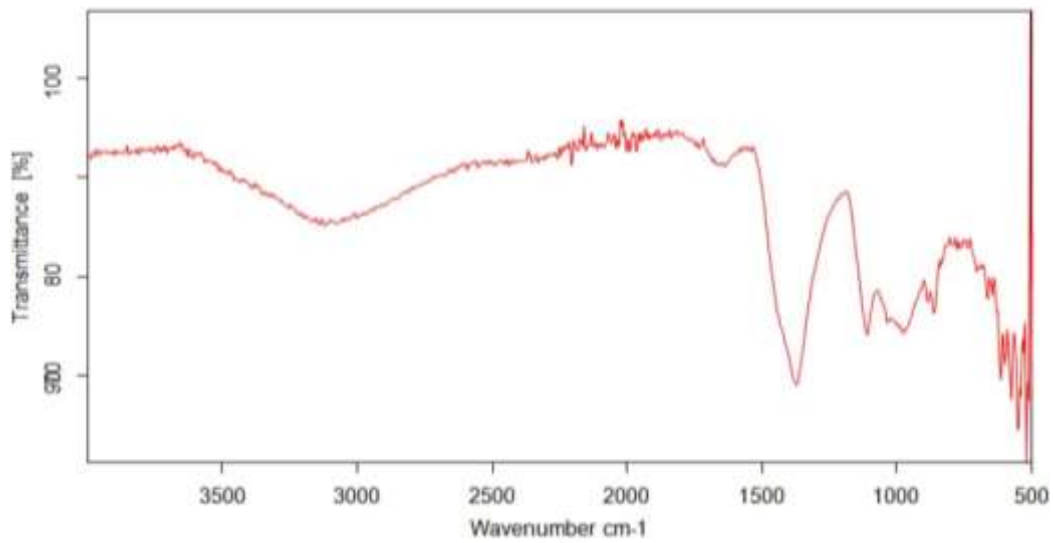
Figure 1: FTIR peaks of the cocoa pods oil
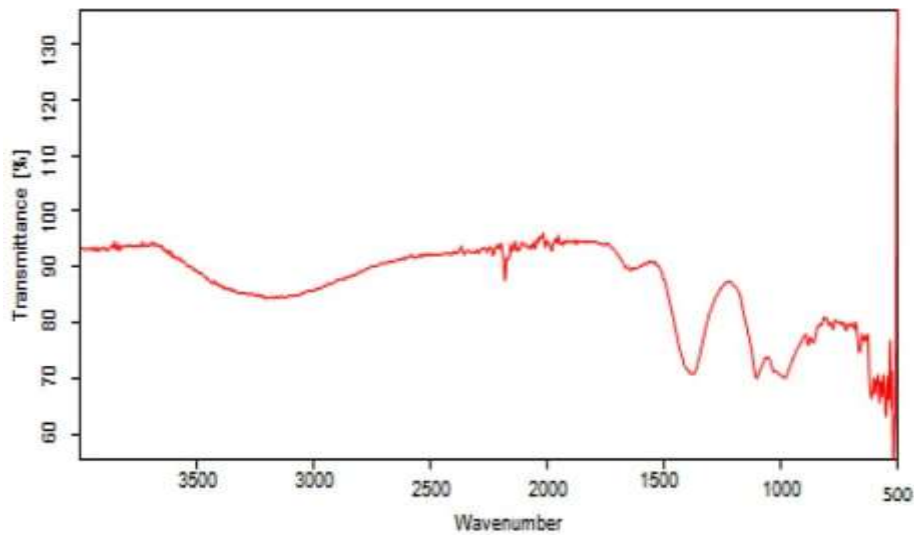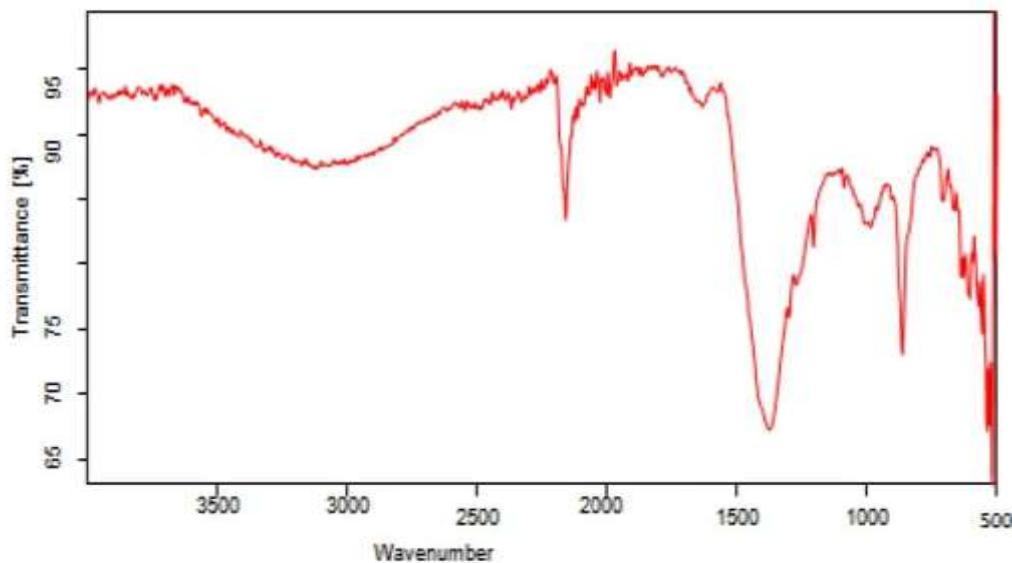

Figure 2: FTIR peaks of palm kernel shell oil

Figure 3: FTIR peaks of the obtained biodiesel from blends of palm kernel shell and cocoa pods oils

3.3.2 Scanning electronic microscopy (SEM)

According to Figure 4, the internal micro-structure, particle size, and shape of the catalyst were ascertained by SEM examination. At a magnification of 80 to 269µm, the majority of the particles were in the nanometer range and had high porosity, indicating a high specific surface area of the catalyst. The shape of the nanocatalyst was made up of closely spaced particles with improved active sites, increased surface area, and high porosity.
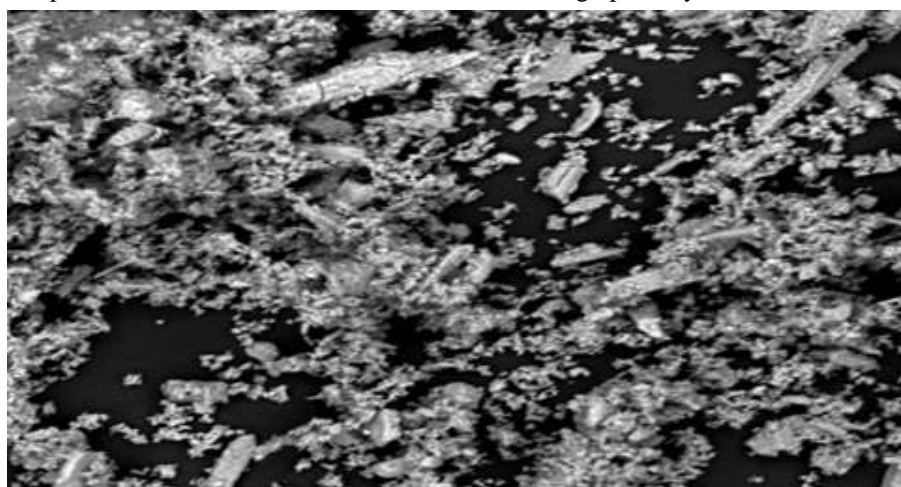
Figure 4: SEM micrograph of the Nano catalyst

3.3.3 Gas chromatography- mass spectroscopy (GC-MS)

The different chemical components found in the oils and biodiesel were identified and quantified using the GC-MS analysis, as shown in Figures 5 to 7. The NIST MS software was used to determine this. The biodiesel chromatogram displays the analysis conducted in the study to verify the biodiesel's conversion in the presence of various methyl esters found in blends of palm kernel shell oil and cocoa pods. Methyl linoleate accounted for 63.031% of the total methyl esters, followed by methyl palmitate (26.7%), methyl oleate (8.1%), and methyl eicosadinoate (2%).

3.3.4 X-ray Diffraction Analysis (XRD)

The TiO_2 anatase structure is confirmed by the 2-theta at a peak of 25.4°. Strong diffraction peaks indicate that TiO_2 is in the anatase phase at 25° and 48°. The sample has no discernible diffraction peak. The anatase structure of the 2-theta peaks at 25.27° and 48.01° is confirmed. Broad diffraction peaks suggest very small-sized crystallites, and the sample's strength of XRD peaks indicates that the produced nanoparticles are crystalline.

3.5 Characterization of the Biodiesel blends and Diesel Fuels

The biodiesel as produced from the palm kernel and cocoa pod oils; and blended with the fossil diesel at different volumes, such as B_{10}, B_{20}, B_{30}, B_{40} and B_{100} including the one hundred percent (100%) fossil diesel (D_{100}) were

characterized in order to ascertain their fuel properties. The results of the characterization shown in Tables 4 and 5, are presented in the pie charts.

3.5.1 Kinematic viscosity

The fluid parameter that characterises the impact of shear stress on the fluid is called kinematic viscosity. Less viscous fuels burn more efficiently than highly viscous fuels, according to studies. Fuels with viscosities over the specified limit increase the possibility of partial combustion, exhaust emission pollution, filter damage, and excessive pump resistance [18].

According to Table 4, the kinematic viscosity range for the samples shown in Figure 9 is 5.21 to 7.78 mm^2s^{-1}. The kinematic viscosity limit set by the Agency for Petroleum, Natural Gas & Biofuels (ANP) is 1.9 - 6.00 mm^2s^{-1}. Based on the results, D_{100} and B_{10} mixes are within the range; however, other blends are also within acceptable bounds. The viscosity of the diesel fuel determines how it atomizes. This suggests that fuel atomization rises as fuel viscosity decreases.
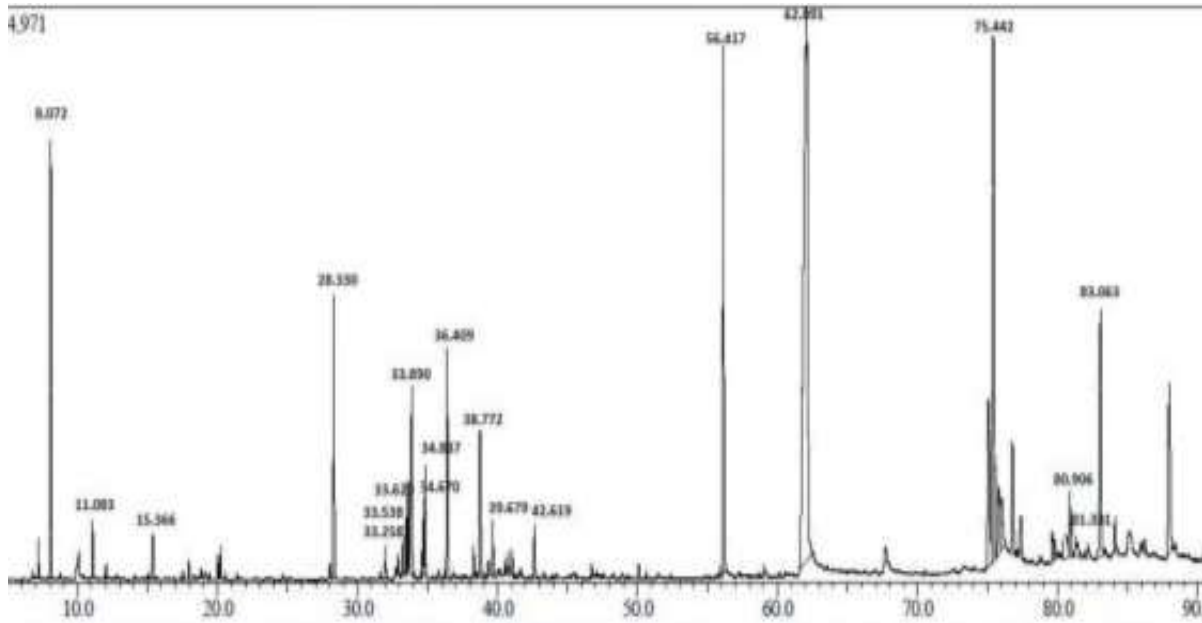
Figure 5: GC-MS analysis for cocoa pods methyl esters extraction
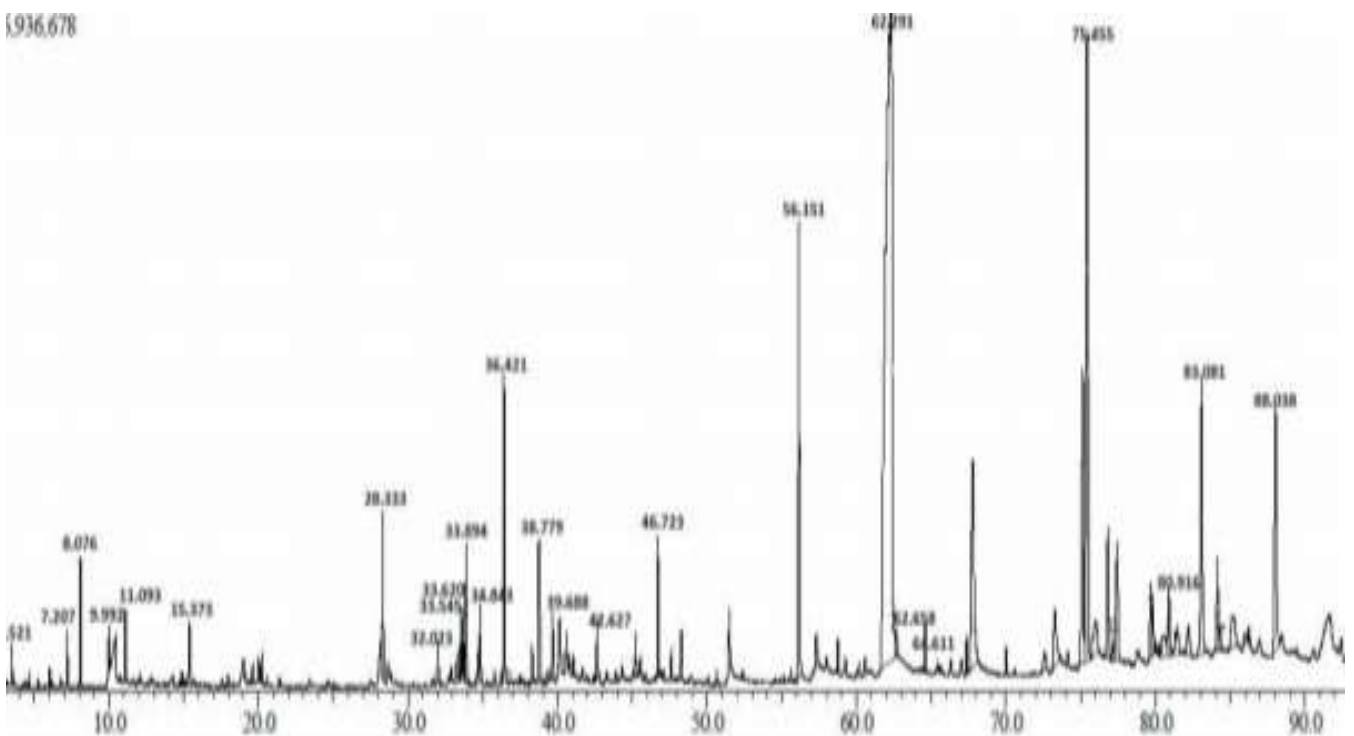
Figure 6: GC-MS analysis for palm kernel shell methyl esters extraction
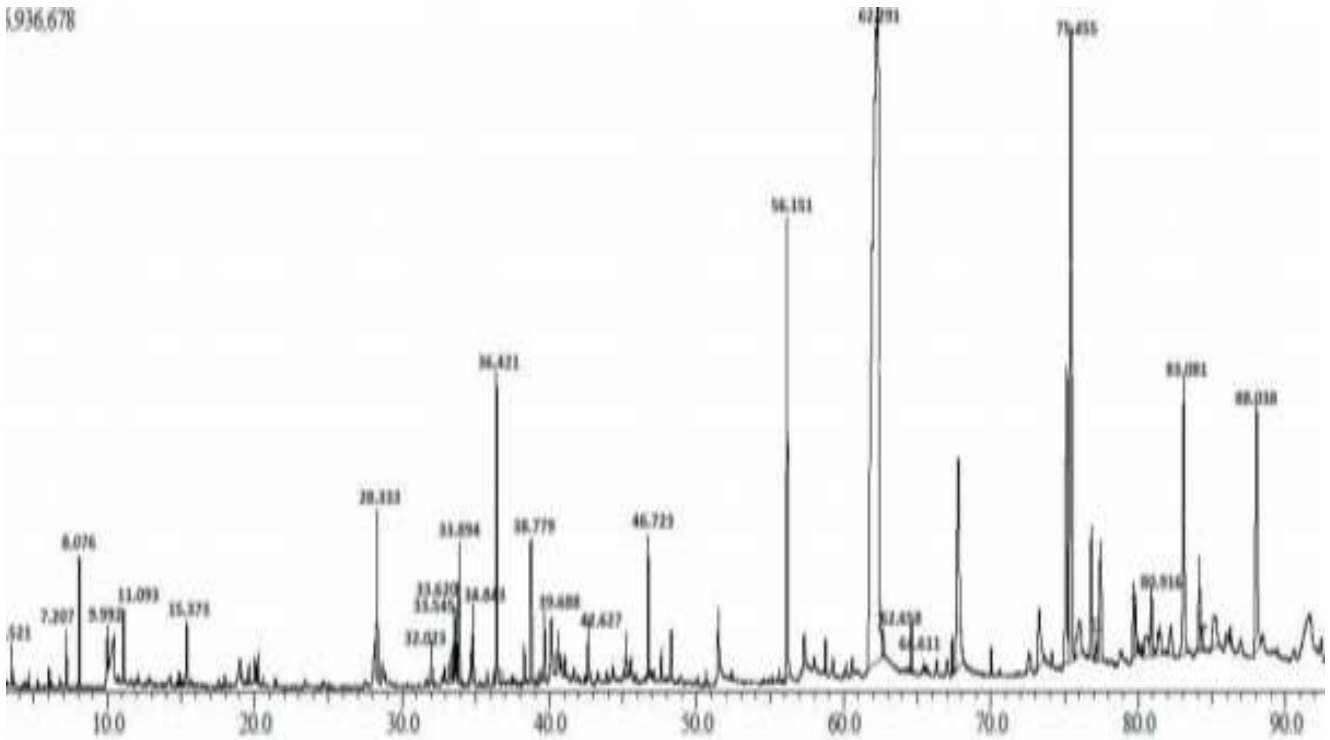
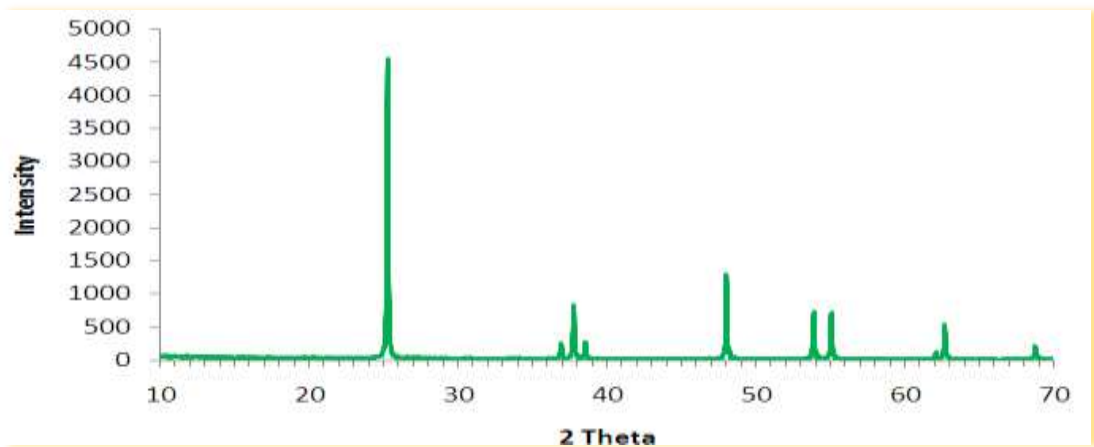Figure 7: GC-MS blends of cocoa pods and palm kernel shell methyl esters

Figure 8: XRD pattern of TiO_2 nanoparticles

Table 4: Characterization of the biodiesel (blends) and fossil diesel

Sample Id.	Viscosity @ 40^0C (mm^2s^{-1})	Density (Kg/m^3)	Flash point (^0C)	Fire point (^0C)	Cloud point (^0C)	Pour point (^0C)
D_{100}	5.21	0.8351	96.56	107	3.91	1.5
B_{10}	5.65	0.8428	101.72	108	4.48	2
B_{20}	6.41	0.8511	101.68	112	4.51	2
B_{30}	6.98	0.8599	102.56	114	4.62	2.5
B_{40}	7.21	0.8621	107.68	118	4.73	2.5
B_{100}	7.78	0.8642	140.79	150	6.48	4.5

Table 5: Characterization of the biodiesel (blends) and fossil diesel (contd)

Sample Id.	Acid value (mg KOH/g)	Anisidine Point (^{0}c)	Diesel index	API Gravity	Cetane Number	Gross calorific value (J/g)
D_{100}	**0.911**	53	44.23	34.55	40.91	7263.68
B_{10}	**0.841**	50	41.45	32.89	37.78	7443.67
B_{20}	**0.676**	49	40.11	32.65	37.34	7671.24
B_{30}	**0.651**	48	38.54	32.33	36.76	7825.33
B_{40}	0.573	47.67	37.78	31.54	35.98	7960.44
B_{100}	**0.348**	46	32	29	30.13	8063.53

.
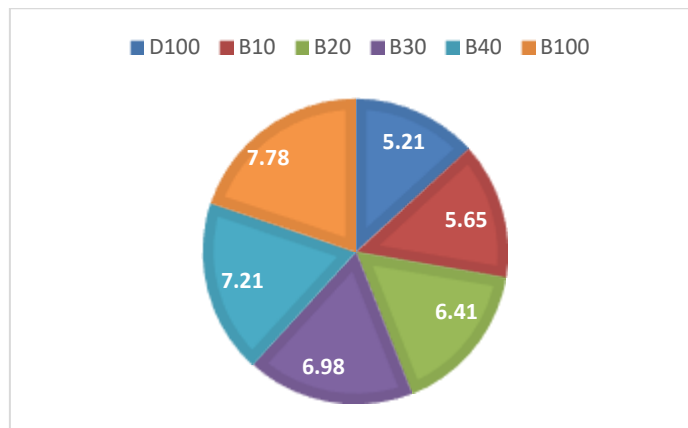
Figure 9: Optimal yield on kinematic viscosity at 40^0C (mm^2s^{-1}) of the biodiesel (blends) and diesel

3.5.2 Density

Figure 10 presents the biodiesel yields on density with the blends. The density of the petroleum diesel as presented in Table 4 is lower than the blends and the pure biodiesel from the palm kernel shell and the cocoa pod oils. This is consistent with the report done by other research works [47] From the Table 4, the observed densities ranged from 0.8351 to 0.8642 kg m^{-3}.

Densities of the petroleum diesel, blends and the pure biodiesel from which the blends were formed gradually increased. When contrasted with petroleum diesel, the blends and pure biodiesel with their higher density had an advantage. This is referred to as being 'chemically advanced', because it modifies the injection time [49]. This phenomena indicates that, in comparison to petroleum diesel, the time needed for biodiesel and its blends to move from the injection pump to the injector was significantly less. This effectively makes up for biodiesel's lower energy value [47]. The densities attained in this work fall between the 0.860 - 0.900 kg m^{-3} range that is allowed by EN.
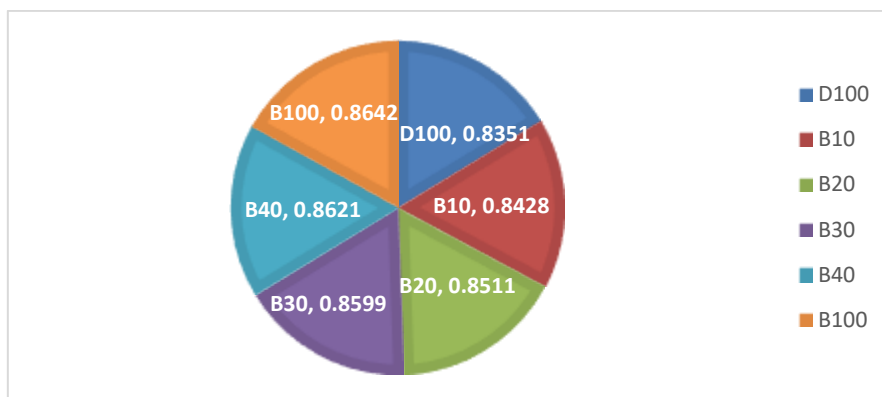

Figure 10: Optimal yield on density of the biodiesel (blends) and diesel

3.5.3 Flash point

Fuel heat properties, such as flash point and fire point, specify the maximum safe temperature at which a fuel can be exposed without combusting when a light source is brought close to it. These characteristics are also thought to be safe fuel storage attributes. As shown in Figure 11 and presented in Table 4, the research findings on the fuel qualities of biodiesel derived from palm kernel and cocoa pod oils indicate that the flash point values fall between 96.56 and 140.79^{0}C. The EN14214 biodiesel specification for B_{100} is > 120^{0}C.
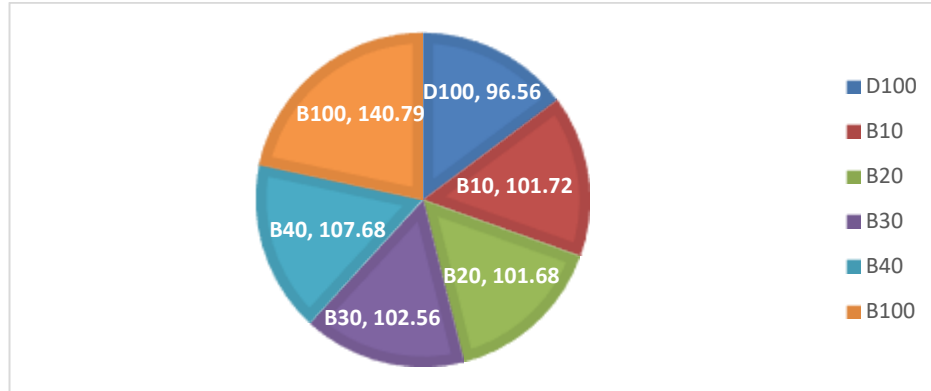
Figure 11: Optimal yield on flash point of the biodiesel (blends) and diesel

3.5.4 Fire point

The results obtained for the fire point ranged from 107 - 150^{0}C, as shown in Figure 12 and presented in Table 4. The fuel with the lowest fire and flash points is diesel. Thus, the biodiesel fire point increases as the blend ratio increases. The EN standard states that 120^{0}C is the minimum flash point value for unblended biodiesel. Ideally, flash point values should be lower than fire point values.
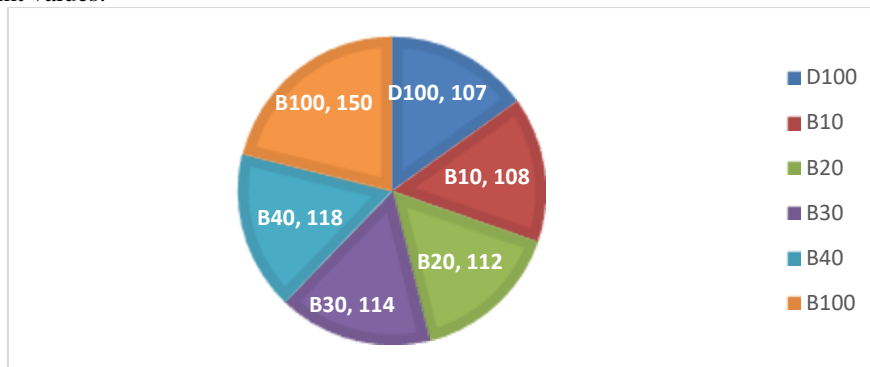

Figure 12: Optimal yield on fire point of the biodiesel (blends) and diesel

3.5.5 Cloud point

Fuel cold flow parameters such as cloud point and pour point are used to estimate the potential viscosity of liquid fuel at low temperatures. These fuel characteristics include storage capabilities in addition to flash and fire points. Figure 13 shows the results for the optimal biodiesel yield on cloud point as presented in Table 4. The cloud point values ranged from 3.91 – 6.48^{0}C. The basic standard for biodiesel fuel cloud point is -3 to 15^{0}C. The results obtained are within the acceptable range of this standard.
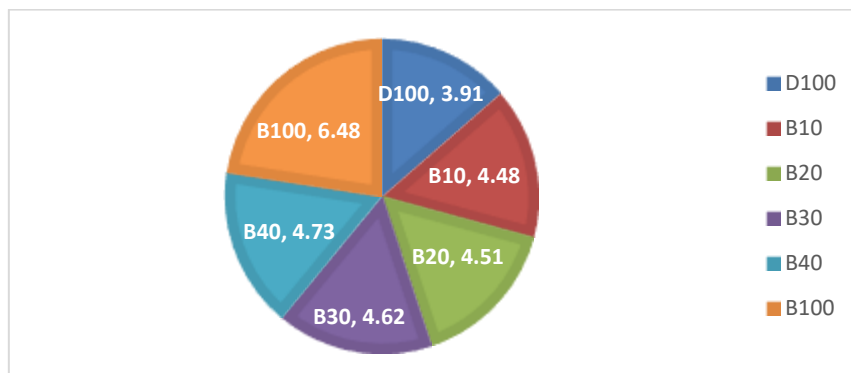.

Figure 13: Optimal yield on cloud point of the biodiesel (blends) and diesel

3.5.6 Pour point

The lowest temperature at which a liquid fuel solidifies into a bulk is known as the pour point. From the Table 4, diesel fuel has the lowest pour point, with B_{10}, B_{20}, B_{30}, B_{40}, and B_{100} following closely behind. The pour point standard range set by ASTM is between -5 and 10^0C. As seen in Figure 14, the range of values obtained for the pour point is 1.5 to 4.5^0C. These values are within the acceptable range.
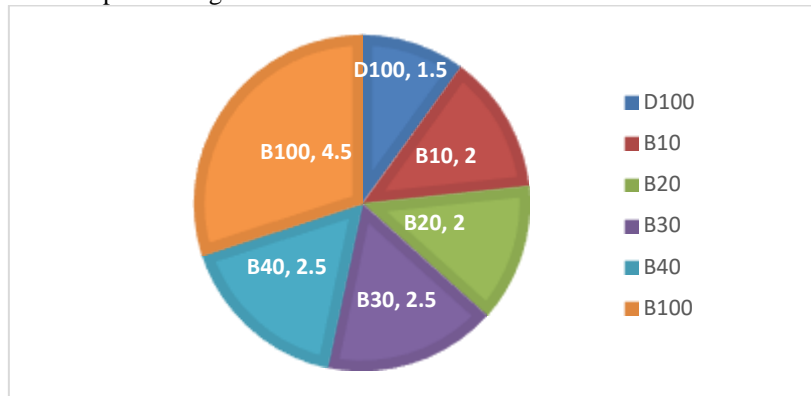

Figure 14: Optimal yield on the pour point of biodiesel (blends) and diesel

3.5.7 Free fatty acid (FFA)

The acid value is a fuel storage property, which determines the stability of the fuel. Oxidation of impurities such as metallic filings, and/or corrosion, and phosphates in fuel, due to environment can influence the fuel storage stability. From the results obtained, values for pure diesel fuel (D_{100}) and biodiesel (B_{100}) are 0.911 and 0.348 mgKOH/g respectively. According to Figure 15, as presented in Table 5, the blend values decreased as biodiesel blends increased (B10 < B20 < B30 < B40); and they fall between the values for D_{100} and B_{100}. According EN 14214 biodiesel specification, oxidation stability at 110^0C is Max 0.50 mg/KOH/g.
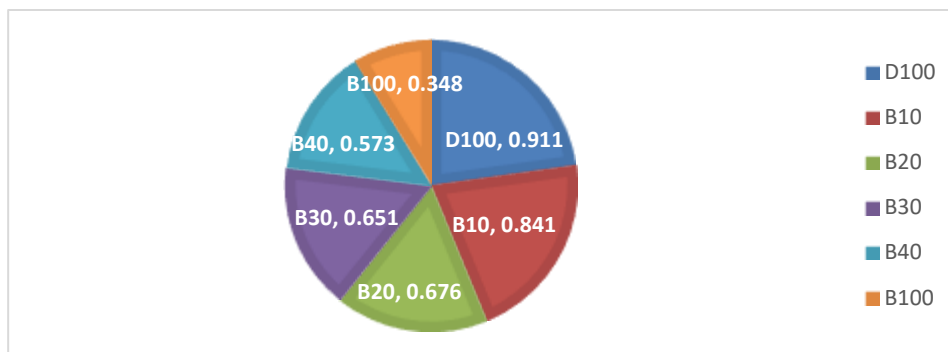

Figure 15: Optimal yield on free fatty acid of the biodiesel (blends) and diesel

3.5.8 Anisidine point

The lowest temperature at which the same quantity of products fully mixes with aniline is known as the fuel's anisidine point. Another name for it is the aromaticity test. Compared to biodiesel, petroleum diesel has a greater aniline point. Products with a lower aniline point have more aromatic hydrocarbons in them [6]. This is because fuels with higher aromatic hydrocarbon content would mix more quickly with aniline. Figure 16 shows an aromatic hydrocarbon with a melting point between 46 and 53^0C. The anisidine point can also be used to determine how much carbon is in a certain fuel [50].
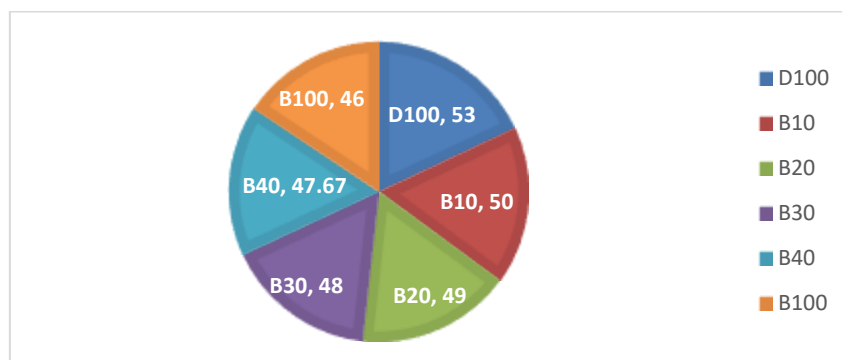

Figure 16: Optimal yield on anisidine of the biodiesel (blends) and diesel

3.5.9 Diesel index

A fuel's ability to ignite is measured by its diesel index [50]. In contrast to the biodiesel, Table 5 shows that the petroleum diesel has a higher ignition quality. Similarly, blends with lower percentages of biodiesel have greater diesel index ignition qualities, which range from 41.45 to 44.23 (Figure 17). According to EN specification, a good diesel index range between 40 – 55 [58]. B_{20}, B_{10} and D_{100} fall within the range.
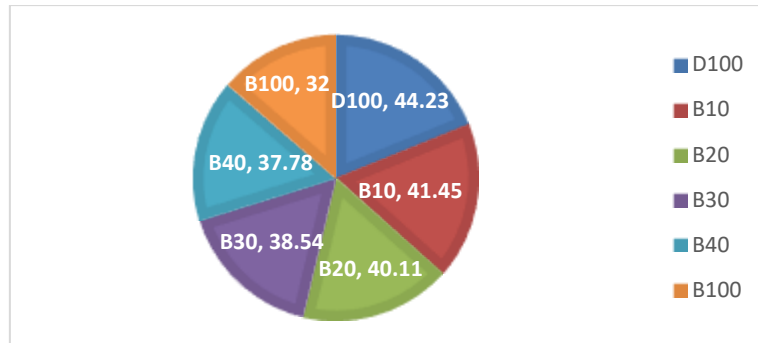

Figure 17: Optimal yield on diesel index of the biodiesel (blends) and diesel

3.5.10 America Petroleum Institute (API) gravity

Figure 18 presents the optimal yield on API of the biodiesel and its blends with the petroleum diesel. The blends and pure biodiesel made from the oils from palm kernel shells and cocoa pods have lower APIs than the petroleum diesel, as seen in Figure 18 and Table 5. An indicator of a fuel's weight in respect to water is the API gravity. This refers to the fuel's potential weight. From the EN standard, value that is more than 10 indicates that the fuel is lighter than water and will float on it; but value less than 10 indicates that the fuel is heavier and will sink in water. From the results obtained in this work, the API gravity ranged from 29 for unblended biodiesel to 34.55 for 100% petroleum diesel. This is in line with the EN standard since all values obtained are greater than 10.
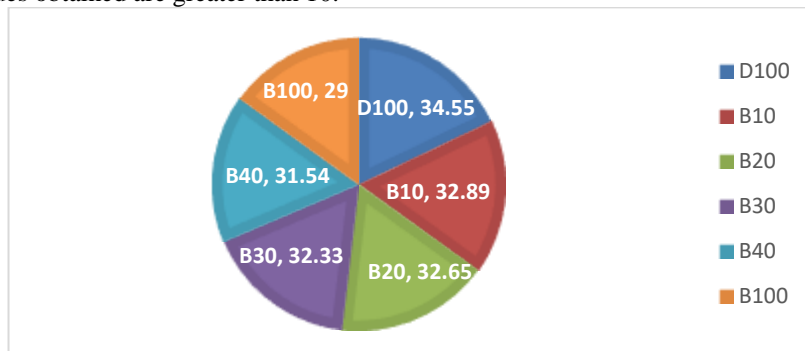

Figure 18: Optimal yield on API gravity of the biodiesel (blends) and diesel

3.5.11 Cetane number

A dimensionless fuel quality metric called cetane number is essential for determining whether the fuel is suitable for combustion in a compression ignition engine [47]. A biodiesel fuel with a higher cetane number will burn more efficiently. According to this study, pure biodiesel (B_{100}) has a lower cetane number (30.13) than the petroleum diesel (D_{100} = 40.91). As the volume of the biodiesel increases ($B_{10} - B_{40}$), the values for blends decreases (37.78 – 35.98) respectively as shown in Figure 19 and presented in Table 5.
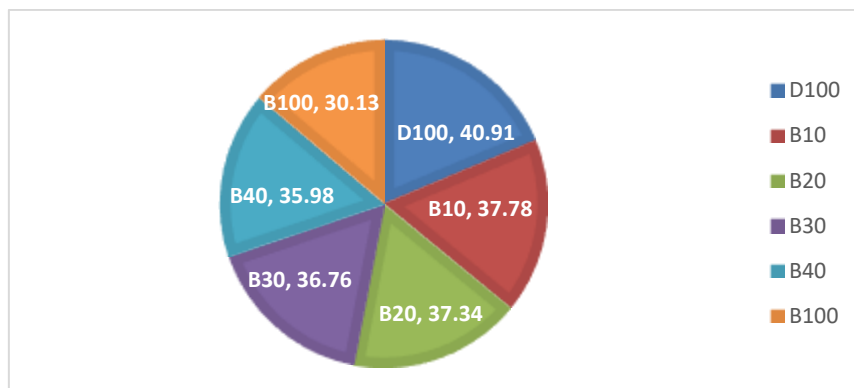

Figure 19: Optimal yield on cetane number of the biodiesel (blends) and diesel

3.5.12 Gross calorific value

Whenever fuel is burnt, heat is released. The amount of heat released depends on different factors, and the fuel burnt. This amount of heat that is developed when a mole of biodiesel is burnt is known as the gross calorific value of the fuel. It is also known as the high heating value of fuel [50]. In this report, the pure biodiesel (B_{100}) has a higher calorific value to the conventional diesel fuel (D_{100}) with values of 8063.53 and 7263.68 J/g respectively as shown in Figure 20 and presented in Table 5. The result obtained is in line with Samuel (2023), where the gross calorific value was 8032.62 J/g for B_{100} and 7373.62 J/g for D_{100}. The values reduced as biodiesel blends reduced.
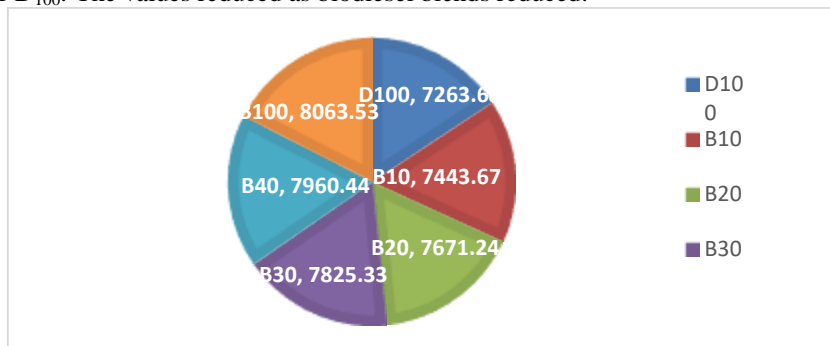

Figure 20: Optimal yield on gross calorific of the biodiesel (blends) and diesel

4. CONCLUSION

Blend of palm kernel shell and cocoa pods oils was successfully used for the production of biodiesel with titanium oxide as catalyst. Before blending, the individual oils were extracted and characterized. Results of 4 and 1.76 mEq/kg for peroxide value, 36 and 42.1 mg/100g for iodine value, 0.861 and 0.97 for specific gravity, 190 and 229.6 mgKOH/kg for saponification, 16.7 and 18.83% of oil yield etc. were obtained for cocoa pods and palm kernel shell oils respectively. For the blend, specific gravity of 0.94, energy value of 140.5 kJ/kg, Density of 0.878 g/ml, saponification value of 194 mgKOH/kg, peroxide value of 3.7 mEq/kg, moisture content of 1.16% etc. were also obtained. Utilising a titanium oxide nanocatalyst, the extracted blend was used to transesterify methanol. The catalyst shape, particle size, and internal microstructure were all determined by SEM analysis. The shape of closely spaced particles with improved surface area, better active sites, and high porosity is displayed in the result. The oil blend was successfully converted to biodiesel using the titanium oxide catalyst. The produced biodiesel was characterized by fire point, pour point, cetane index, cloud point, acid value, API gravity, gross calorific value etc., in accordance with the ASTM Standard range, EN, and ANP defined limit for diesel fuels. Findings were within the recommended threshold. ANP stated limit, EN, and ASTM Standard range for diesel fuels were also used to determine the properties of the produced biodiesel, the blends, and the best blend properties, compared to the conventional (fossil) diesel. In the comparison with the fossil diesel (D_{100}), pure biodiesel (B_{100}) and its blends (B_{10}, B_{20}, B_{30}, and B_{40}) were utilised. Kinematic viscosity, density, fire point, cloud point, and gross calorific values all increased as the biodiesel blends increased. On the other hand, as the blend volume increased, the acid value, cetane number, anisidine point, diesel index, and API gravity decreased. These results demonstrate that blending of the oils from palm kernel shells and cocoa pods can be employed in the production of efficient biodiesel. Additionally, titanium oxide can be utilised as a catalyst due to its properties and notable effects on the yield of biodiesel.

ACKNOWLEDGMENT

REFERENCES

[1] Agarwal, A. K. (2007). Biofuels (Alcohols and Biodiesel) Applications as Fuels for internal Combustion Engines. *Prog Energy Combust. Sci.*, 33(1), 233-271.

[2] Meher, L. C., Vidya Sagar, D. & Naik, S. N. (2006). Technical Aspects of Biodiesel Production by Transesterification – A Review. *Renewable Sustainable Energy Review,* 10(1), 248-268.

[3] SLOCAT (2023). Transport, Climate and Sustainability Global Status Report – 3rd edition. www.tcc-gsr.com. – Sustainable Low Carbon Transport (SLOCAT).

[4] Samuel O. E., Fidelis I. A., Precious O. E., Thomas O. M., Emmanuel E. J., Olusegun D. S., Burhan S, Macmanus C. N., Christopher C. E., Muhammad L. R., & Muji S., (2024). Cost, Estimation and Thermo-Physical Determination of Heterogeneous Biodiesel from Palm Kernel Shell Oil: Optimization of Tropical Egg Shell Catalyst. *Indonesian Journal of Science and Technology*, 9(1), 1–32.

[5] European Environmental Agency (EEA) Report. Modified: 23 May, 2024. https://ozone.unep.org/ozone-and-you[#]:~:text/

[6]   Samuel, O.E (2023). Effects of Process Parameters on Biodiesel Yield Produced from Palm Kernel Shell Oil (PKSO) using Eggshell as Catalyst (2023). *International Journal of Frontiers in Engineering and Technology Research*, 04(01), 001–017.

[7]   Kusdiana, D. & Saka S. (2004). Effects of Water on Biodiesel Fuel Production by Supercritical Methanol Treatment. *Biodiesel Resources Technological Journal*, 91, 289-295.

[8]   Agbede, O. O. (2012). Evaluation of Chosen Fruit Seed Oils as Potential Biofuel. *Journal International Agrophysics*, 26(2), 199-202.

[9]   Butler, R. A. (2006). Why is Oil Palm Replacing Tropical Rainforests? Why are Biofuels Fueling Deforestation? April 25, 2006

[10]   Okoji, A. I., Anozie, A. N., Omoleye, J. A., Taiwo, A. E., & Babatunde, D. E., (2023). Evaluation of Adaptive Neuro-Fuzzy Inference System-Genetic Algorithm in the Prediction and Optimization of Nox Emission in Cement Precalcining Kiln. *Environmental Science and Pollution Research Article*, 30, 54835 – 54845.

[11]   Emberson L. (2020). Effects of Ozone on Agriculture, Forests and Grasslands. *Review articles,* https://doi.org/10.1098/rsta.2019.0327.

[12]   Ahmia, A. C., Danane, F., Bessah, R. & Boumesbah, I. (2014). Raw Materials for Biodiesel Production. Valorization of Used Edible Oil. *Revue des Energies Renouvelables,* 17(2), 335–343

[13]   Hiwot, T. (2018). Mango (Magniferaindica) Seed Oil Grown in Dilla Town as Potential Raw Material for Biodiesel Production using NaOH- a Homogeneous Catalyst. *Chemistry International*, 4(40), 198-205

[14]   Keera, S. T, El Sabagh S. M & Taman (2018). Castor Oil Biodiesel Production and Optimization. *Egyptian Journal of Petroleum,* 27(1), 979-984.

[15]   Ogunsuyi, H. O. (2012). Acid and Base Catalysed Transesterification of Mango [MangiferaIndica] Seed Oil to Biodiesel. *IOSR J. Appl. Chem.*, 2(2), 18-22.

[16]   Syed, A. B., Gopal, K. R. & Jebaraj, S. (2008). A Review on Biodiesel Production, Combustion, Emissions and Performance. *Renewable and Sustainable Energy Reviews,* 13(1), 1628 –1634.

[17]   Montefri, M. J. & Obbard, J. P. (2010). The Economic of Biodiesel Derived from Waste Cooking Oil in the Philippines. *Energy Sources, Part B. Economic, Planning and Policy*, 5(4), 337-347.

[18]   Roa, G. N, Ramadhas, A. S, Nallusany N, & Sakthvei P. (2010). Relationships among the Physical Properties of Biodiesel and Engine Fuel System Design Requirements. *International Journal of Energy and Environment*, 1(5), 919-926.

[19]   Savariraj, S., Ganapathy, T. & Saravanam, C. G. (2011). Experimental Investigation of Performance and Emission Characteristics of Mahua Biodiesel in Diesel Engine. *Renewable Energy*, 20(11), 1-6.

[20]   Agunbiade, F. O., & Adewole, T. A. (2014). Methanolysis of Carica Papaya Seed Oil for Production of Biodiesel. *Journal of Fuels*, 2014(8), https://doi.org/10.1155/2014/904076.

[21]   Rafaat, A. A. (2010). Different Techniques for the Production of Biodiesel from Waste Vegetable Oils. *International Journal of Environmental Sciences and Technology*, 7(1), 183

[22]   Pugazhvadivu, M. & Sankaranarayanan G. (2010). Experimental Studies on a Diesel Engine using Mahua Oil as Fuel. *Indian Journal of Science and Technology*, 3 (7), 787-791.

[23]   Lotero, E, Lui Y, Lopez, D. E, Suwannakara K, Bruce, D. A & Goodwin-Jr J. G. (2005). Synthesis of Biodiesel via Acid Catalyst. *Ind. Eng. Chem. Res.,* 44(14), 5353-5363.

[24]   Fadhil, A. (2013). Optimization of Transesterification Parameters of Melon Seed Oil. *International Journal of Clean Energy*, 10(7), 763-774.

[25]   Claudia C., Leonardo D., & Renzo L. (2019). Titanium Dioxide as a Catalyst in Biodiesel Production. *Review*, 9 (1), 75. https://doi:10.3390/catal9010075.

[26]   Falowo, O. A., Oyekola, O. O., & Davies, O. (2023). Synthesis of Sulfonated Magnetic Nano-Catalyst using Thermodynamic Study. *Waste and Biomass Valorization Paper,* 15(1), 973 – 987.

[27]   Boerlage, G. D. & Broeze, J. J. (1990). Determination of saponification, Iodine and Peroxide Values. *Progress Report of Volunteer Group for Fuel Research Society of Automotive Engineers*, 21(1), 289-305.

[28]   Boerlage G. D. & Broeze, J. J. (1994). Determination of Cetane Number. *Progress Report of Volunteer Group for Fuel Research Society of Automobile Engineers,* 5(1), 231–232.

[29]   Mendes A. Moura (2011). Production of biodiesel from corn oil and ethanol by homogeneous alkali catalyzed transesterification. *Department of Chemical Engineering, Royal Institute of Technology (KTH) Stockholm, Sweden,* 3(2), 1-47

[30]   Anwar, M., Rasul, M. G., Ashwath, N. & Rahman, M. M. (2018). Optimisation of Second-Generation Biodiesel Production from Australian Native Stone Fruit Oil Using Response Surface Method. *Energies,* 11(2566), 1-18.

[31]   Zhao C. (2018). Biodiesel Synthesis Over Biochar-based Catalyst from Biomass Waste Pomelo Peel. *Energy Conversion and Management,* 160(1), 477–485.

[32]   Quingyun Zhao, Fei Han, Yuhong Huang, Xiaohui She, Zhanpin You, & Biao Zhang (2024). Research of Carbon Footprint Calculation and Evaluation Methods based on the Pattern Microalgae for Biodiesel Production. *Renewable Energy,* 231, 120912.

[33] Rahadianti, E., Yerizam, Y., Martha, M. (2018). Biodiesel Production from Waste Cooking Oil. *Indonesian Journal of Fundamental and Applied Chemistry,* 3(3), 77-82.

[34] Olayomi A. F., Babatunde O., Abiola E. T., Ayomiposi T. O., Oluwaseun O.O., & Eriola B., (2022). Green Heterogeneous Based Catalyst from Ripe and Unripe Plantain Peels Mixture for the Transesterification of Waste Cooking Oil. *Chemical Engineering Journal Advance*, 10(4), 100293

[35] Harabi, M., bouguerra, S., marrakchi, F., & Bouaziz, M. (2019). Biodiesel and Crude Glycerol from Waste Frying Oil: Production, Characterization and Evaluation of Biodiesel Oxidative Stability with Diesel Blends. *Sustainability*, 11(7), 1937

[36] Atadashi, M., Aroua, M., Sulaiman, N., & Raman. (2013). The Effects of Catalysts in Biodiesel Production: A review. *Journal of Industrial and Engineering Chemistry*, 19(1), 14-26.

[37] Agbede, O. O. (2012). Evaluation of Chosen Fruit Seed Oils as Potential Biofuel. *Journal International Agrophysics,* 26(2), 199-202.

[38] Akpaka, P., Igboanugo, A., & Omotehinse, S. (2013). Analysis of some Factors Affecting Production Process of Rubber Seed Oil-based Biodiesel by Opinion Discrimination Analytical Modelling. *J. Appl. Sci. Environ. Manage*, 23(1), 173-178.

[39] Rajarshi K, Oindrila G, & Mukundu K. D. (2012). Biodiesel Production and Process Optimization. *International Journal of Scientific and Research Publications*, 2(6), 2250-3153

[40] Walkley, A. & Black, I.A. (1934). An Examination of the Degtjareff Method for Determining Soil Organic Matter, and a Proposed Modification of the Chromic acid Titration Method. *Soil Sci.,* 37, 29-38.

[41] Velickovic, V., Velickovic, A., Avramovic, J., & Stamenkovic, O. S. (2019). Modelling of Biodiesel Production: Performance Comparison of Box–Behnken, Face Central Composite and Full Factorial Design. *Chinese Journal of Chemical Engineering*, 27(1), 1690-1698.

[42] Shaaban, W., Shazly, A., Elkady, M., & Ohshima, M. (2015). Investigation of Factors Affecting Biodiesel Production in Microreactor with T-Mixer. *International Proceedings of Chemical, Biological and Environmental Engineering,* 88(3), 11-15.

[43] Haryanto, A., & Telaumbanua, M. (2020). Application of Artificial Neural Network to Predict Biodiesel Yield from Waste Frying Oil Transesterification. *Indonesian Journal of Science and Technology*, 5(1), 62-74.

[44] Babajide, O. O. (2011). Optimisation of Biodiesel Production via Different Catalytic and Process Systems. *University of the Western Cape; Thesis,* 1-276.

[45] Keera, S. T., El Sabagh S. M, & Taman A. R. (2018). Castor oil biodiesel production and optimization. Egyptian journal of petroleum, 27(4): 979-984.

[46] Knothe G. (2010). Progress in Energy and Combustion Science. *Peer-reviewed journal,* 36 (2010), 364–373

[47] Ayetor, G. K., Sunnu, A & Parbey, J (2015). Effects of Biodiesel Production Parameters on Viscosity and Yield of Methyl esters: Jathropha curcas, Elaeis guneensis and Cocos nucifera. *Alexander Engineering Journal*, 54, 1285-1290.

[48] Cheng, J. J. & Timilsina, G. R. (2011). Status and Barriers of Advance Biofuel Technologies: A Review. *Renewable Energy*, 36, 3541-3549.

[49] Flavio, C. (2011). Impact of Biodiesel Bulk Modulus on Injection Timing; The Effect of Residual Pressure. *Fuel*s, 90(3), 477-485.

[50] Owolabi R, Osiyemi N. A, Mutui K. A & Elizabeth O. M. (2011). Biodiesel from Household/Restaurant Waste Cooking Oil (WCO). *Journal of Chemical Engineering and Processing Technology*, 2(04), 1-4.

[51] Akinola, A. O., Elche, J. F., Owolabi, P. O., & Elegbeleye, A. P. (2018). Pyrolytic Analysis of Cocoa Pod for Biofuel Production. *Nigerian Journal of Technology (NIJOTECH)*, 3(4), 1026–1031.

[52] Fernando S. D., Jha, S. K., & Tu, S. F. (2007). Flame Temperature Analysis of Biodiesel Blends and Components. *American Society of Agricultural and Biological Engineers (ASAE) Annual Meeting*, 2007

[53] Thangalazhy-Gopakumar, S., Adhikari, S., Ravindran, H., Gupta, R., Fasina, O., Tu, M., & Fernando, S. (2010). Physiochemical Properties of Bio-diesel Production at various Temperatures from Pine Wood using an Auger Reactor. *Bio-resource Technology*, 101(21), 8389–8395

[54] Omojola, A, & Daramy, V.K. (2023). Achieving Affordable and Clean Energy through Conversion of Waste Plastic to Liquid Fuel. *Journal of the Energy Institute*, 106, 101154

[55] Chen, D., Zhuo, J., Zhang, Q., & Zhu, X. (2014). Evaluation Methods and Research Progresses in Bio-oil Storage Stability. *Renewable and Sustainable Energy Reviews*, 40, 66–79.

[56] Mortensen, P. M., Grunwaldt, J. D., Jensen, P. A., Knudsen, K. G., and Jensen, A.D. (2011). A Review of Catalytic Upgrading of Bio-oil to Engine Fuels. *Applied Catalysis A*, 407(1 – 2), 1–19.

[57] Cheng, S., Wei, L., Zhao, X., & Julson, J. (2016). Application, Deactivation, and Regeneration of Heterogeneous Catalysts in Bio-oil Upgrading. *Agricultural & Biosystems Engineering Department, South Dakota State University, 1400 North Campus Drive, Brookings, SD57007, USA*, 6(12), 195.

[58] Anton A. K., Alexandre C. D., Gadi, R. & Sunmonu, M. O. (2008). Solid Acid Catalyst for Biodiesel Production – Towards Sustainable Energy. *American Oil Chemists Society*, 1660, 4-7.